Internal Interface Strains Effects on UO2/U3O7 Oxidation Behaviour

Nicolas Creton, Virgil Optasanu, Sébastien Garruchet, Tony Montesin, Laura
Raceanu, Lionel Desgranges, Steeve Dejardin

HAL Id: hal-00463283
https://hal.archives-ouvertes.fr/hal-00463283

Submitted on 11 Mar 2010

Internal interface strains effects on UO$_2$/U$_3$O$_7$ oxidation behaviour

N. Creton[1,a], V. Optasanu[1, b], S. Garruchet[1,c], L. Raceanu[1,d],

T. Montesin[1,e], L. Desgranges[2,f], S. Dejardin[1,g]

[1]I.C.B., UMR 5209 CNRS, 9 Avenue Alain Savary, B.P. 47870 21078 Dijon, FRANCE

[2]CEA/DEN/DEC/SESC/LLCC, CEA Cadarache, 13115 St Paul lez Durance, FRANCE

[a]nicolas.creton@u-bourgogne.fr, [b]virgil.optasanu@u-bourgogne.fr,
[c]sebastien.garruchet@u-bourgogne.fr, [d]laura.raceanu@u-bourgogne.fr,
[e]tony.montesin@u-bourgogne.fr, [f]lionel.desgranges@cea.fr,
[g]steeve.dejardin@u-bourgogne.fr

Abstract. The growth of a U$_3$O$_7$ oxide layer during the anionic oxidation of UO$_2$ pellets induced very important mechanical stresses due to the crystallographic lattice parameters differences between UO$_2$ and its oxide. These stresses, combined with the chemical processes of oxidation, can lead to the cracking of the system, called chemical fragmentation. We study the crystallographic orientation of the oxide lattice growing at the surface of UO$_2$, pointing the fact that epitaxy relations at interface govern the coexistence of UO$_2$ and U$_3$O$_7$. In this work, several results are given:

- Determination of the epitaxy relations between the substrate and its oxide thanks to the Bollmann's method; epitaxy strains are deduced.

- Study of the coexistence of different domains in the U$_3$O$_7$ (crystallographic compatibility conditions at the interface between two phases: Hadamard conditions).

- FEM simulations of a multi-domain U$_3$O$_7$ connected to a UO$_2$ substrate explain the existence of a critical thickness of U$_3$O$_7$ layer.

Introduction

In order to have a better understanding of mechanisms that govern the chemical fragmentation reaction related to the anionic oxidation of UO$_2$ we propose here to study the relations between mechanical stress and oxygen diffusion in a system composed of U$_3$O$_7$/UO$_2$. This study need:
- to understand the nature of the interface existing between UO$_2$ and U$_3$O$_7$,
- to determine the interfacial stress-free strain tensor activated during the UO$_2$ to U$_3$O$_7$ transformation.

In a first part we study the oxidation front between these two phases, from a purely geometrical point of view. We want firstly to know if there is compatibility between the crystallographic lattices, and secondly to deduce an epitaxial strain tensor. We assume the existence of a coherent interface between the substrate and its oxide, i.e. we consider that the move from the crystallographic lattice of the substrate to the oxide's one is realized, from a crystallographic point of view, through a homogeneous transformation between the initial (substrate) and deformed (oxide) configurations. Two methods are used and compared:
- a first method giving, if it exists, the nature of the crystallographic compatibility at the interface (Hadamard condition [1], [2]),
- a second one giving a good coincidence criterion between the crystallographic phases (Bollmann's method) allowing to know the relative orientation of the oxide regarding the substrate, but also the induced strain value necessary to arrange the crystallographic lattices (epitaxy strain).

Furthermore, we compute using a FEM code the stress due to the connection between lattices of UO_2 and U_3O_7 and the diffusion of oxygen atoms in UO_2 using a coupled chemical / mechanical model. We will show that the thickness of U_3O_7 layer has an influence on the maximum stress inside this one, beyond which the layer cracks.

Physical parameters.

In the table below are given the parameters used in the different calculations and simulations presented in this paper.

	D_1 [cm^3/s]	η_{ij}^1/ρ	T [°C]	E [GPa]	ν	Lattice parameters [Å]		
						a	b	c
Ref.	[3]	[4]		[5]		[6,7]		
UO_2	$0.0055\exp\left(\dfrac{-26.3}{RT}\right)$	$-1.248.10^{-5}$	300	200	0,32	5,47 (cubic)		
U_3O_7						5,40 (tetragonal)		5,49

Table 1. Parameters of UO_2 and U_3O_7.

Study of the epitaxy relations between a substrate UO_2 and its oxide U_3O_7

Hadamard condition. In the case of a homogeneous transformation between two configurations (initial and deformed), we define, at any instant t, a vector function Φ written as an affine correspondence between two vectors $\vec{X}$ and $\vec{x}$ of a particle in the two configurations:

$$\vec{x} = \underline{F}(t)\vec{X} + \vec{c}(t).\tag{1}$$

$\underline{F}(t)$ is the transformation gradient in M_0 given by $\underline{F}(t) = \nabla\Phi(\vec{X},t)$, with det($\underline{F}(t)$)>1. $\underline{F}(t)$ allows to link an elementary vector $\vec{X}$ describing M_0 in the initial configuration to its counterpart $\vec{x}$ in the deformed configuration. If we consider two domains Ω_1 and Ω_2 separated by a plan (normal $\vec{n}$) and undergoing continuous displacements, it must exist a condition on these ones, called compatibility condition at the interface, describing the fact that the two linear deformations inside each domain have a coherent interface whereas the gradients of these deformations are different both side of the interface (i.e. the two strains are different). In this way, let's consider the gradients ($\underline{F}_1(t)$ and $\underline{F}_2(t)$) of the homogeneous transformations in the two domains Ω_1 and Ω_2: these gradients are defined in each domain, using Eq. 1. The two corresponding equations have to be verified, at the same time, for any point of the interface (i.e. the two position vectors $\vec{x}_1$ and $\vec{x}_2$ are the same at the interface). These equalities lead to introduce a vector $\vec{a}$ corresponding to the difference between the transformations of vector $\vec{n}$ both side of the interface. We obtain then [2]:

$$\underline{F}_1(t) - \underline{F}_2(t) = \vec{a} \otimes \vec{n}.\tag{2}$$

This equality corresponds to the compatibility condition at the interface (Hadamard condition). From a purely crystallographic point of view, for phases whose lattices are different, this condition allows to know if these phases are compatible, i.e. can coexist on each side of a coherent interface.

We applied this condition to the case of a U_3O_7 oxide layer with a (010) direction parallel to a (001) direction of a UO_2 substrate, perpendicular to the interface. We show that:

- a perfect interface between the substrate and the oxide can not exist a priori (there is no geometrical compatibility between the crystallographic lattices of UO_2 and U_3O_7).

- a perfect interface can exist between two U_3O_7 domains of different crystallographic orientations (possibility to obtain the coexistence of U_3O_7 domains): the principal axes of the lattices are then 90°-oriented relative to each other.
- A coherent but no perfect interface can exist between UO_2 and a mixture of two U_3O_7 domains of different crystallographic orientations separated by a perfect interface. The principal axes of the U_3O_7 lattices are oriented in the same direction than the ones of UO_2.

Epitaxial strains: Bollmann's method. This method [8] is used to determine epitaxial strains generated by the growth of an oxide on the surface of a polycrystalline strongly textured metallic substrate. Our work uses some theoretical results obtained by Salles-Desvignes [9] in our lab few years ago. This geometrical approach takes into account the position of lattice points. Let's consider a substrate "1" and its oxide "2" superimposed. To establish a criterion of the best fit between these two lattices, Bollmann interpenetrates their lattices and calculates, for each orientation of the oxide in relation to the substrate, the matrix of linear transformation $\underline{A}$. Mathematically, we can write:

$$\vec{X}_2 = \underline{A}.\vec{X}_1 . \tag{3}$$

Where $\vec{X}_1$ and $\vec{X}_2$ represent the primitive unit cells of the substrate and its oxide, respectively. Then, matrix $\underline{A}$ must verify the complete coincidence of the two lattices. Bollmann then generates the "O" lattice, constituted by the lattice points verifying Eq. 3. In this case:

$$(\underline{I} - \underline{A}^{-1}).\vec{X}_0 = \vec{b} . \tag{4}$$

in which $\vec{X}_0$ is the representative matrix of the "O" lattice and b represents the translation coordinate system of the substrate lattice. So the matrix $\underline{A}$ is related to the primitive unit cell volumes V_b and V_O of the "b" and "O" lattices respectively. Indeed, Eq. 4 gives:

$$\det(\underline{I} - \underline{A}^{-1}) = V_b / V_0 . \tag{5}$$

From the "O" lattice, it is possible to define a "O" cell, which contains points of the substrate and oxide lattices in nearest coincidence. So, the greater the volume of V_O, the more numerous the lattice points in nearest coincidence and consequently better is the fitting between the substrate and its oxide. As V_b is constant, V_O is in the inverse ratio to $\det(\underline{I}-\underline{A}^{-1})$. Then, a criterion of best fit between the two lattices can be given by: *the orientation of optimal coincidence between two lattices corresponds to the minimal determinant value of ($\underline{I}-\underline{A}^{-1}$), A being the matrix of linear transformation from one lattice to the other*.

Such a method is limited to very neighboured lattices (shape and size). In the case of distant lattices, Bonnet [10] generalized this method, replacing the "O" lattice by a "C" lattice, and the "b" lattice by a "B" lattice. These two new lattices can no longer be primitive. In the substrate and oxide lattices, let's consider two multiple lattice cells M_1 and M_2 in good coincidence. A new parameter has to be introduce: the density ratio Σ_1 (resp. Σ_2) corresponding to the multiplicity of M_1 (resp. M_2). So, the determinant of the matrix ($\underline{I}-\underline{A}^{-1}$) is equal to the ratio V_{Mb}/V_{Mc}, where V_{Mb} and V_{Mc} are the multiple lattice cell volume of "B" and "C" lattices. By comparison with Eq. 5, Bonnet writes:

$$\det(I-A^{-1})=V_{Mb}/V_{Mc}. \tag{6}$$

By introducing V_c (volume of the "C" cell), V_1 (primitive unit cell volume of the substrate such as $V_1=V_{M1}/\Sigma_1$) and V_2 (primitive unit cell volume of the oxide such as $V_2=V_{M2}/\Sigma_2$), one obtains:

$$V_c = \frac{V_1 V_2}{\det(\underline{I} - \underline{A}^{-1}).\det U_2} . \tag{7}$$

In this expression, $\det U_2 = V_{M2}$. Consequently, we can generalize the coincidence criterion by the following condition: "$\det(\underline{I}-\underline{A}^{-1}).\det U_2$ has to be minimal". For each orientation of the oxide in relation with the substrate, the computed transformation matrix A has to verify the criterion previously defined: the favored orientation of the oxide is the one that gives a minimal value of the criterion. A radar graph is then drawn and allows to determine the orientation of nearest coincidence. Furthermore, a value of the epitaxial strain tensor is determined using a classical Lagrange's definition for a macroscopic deformation.

In order to complete the results obtained previously and concerning the Hadamard condition, we applied first the criterion to the case of a U_3O_7 oxide layer with a (010) direction parallel to a (001) direction of a UO_2 substrate: the corresponding radar graph is given in Fig. 1a. We observe that the two lattices are in near coincidence if their principal axes are superimposed (0° between the two lattices with a symmetry of 90°).

In the case of a U_3O_7 oxide layer with a (100) direction parallel to a (111) direction of a UO_2 substrate, what was proposed by Allen for a UO_2/U_3O_8 system, the graph is given in Fig. 1b. The favored orientation of the oxide is then obtained for an a_{U3O7} axis oriented at 40° to an a_{UO2} axis.

$$\varepsilon_{\text{epitaxy}} = \begin{bmatrix} 0.01305 & -0.02562 & -0.00042 \\ -0.02562 & 0.01433 & -0.00002 \\ -0.00042 & -0.00002 & -0.00364 \end{bmatrix} \qquad \varepsilon_{\text{epitaxy}} = \begin{bmatrix} -0.23487 & 0.23347 & -0.05195 \\ 0.23347 & -0.18376 & -0.01989 \\ -0.05195 & -0.01989 & 0.105173 \end{bmatrix}$$
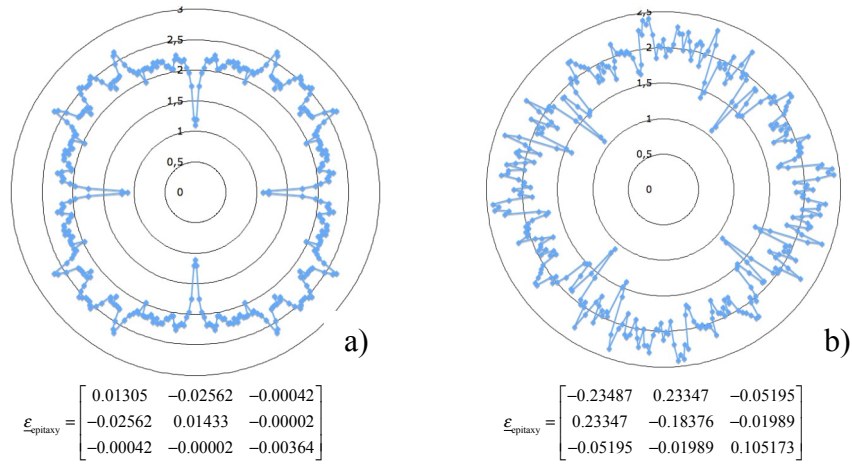
Fig. 1. Radar graph of nearest coincidence criterion vs orientation of U_3O_7 in relation with UO_2: a) $(010)_{U3O7}$ parallel to $(100)_{UO2}$; b) $(100)_{U3O7}$ parallel to $(111)_{UO2}$.

Modelling of a U_3O_7 layer on UO_2

In order to highlight the chemical and mechanical coupling behaviour we will calculate the mechanical stress and the concentration of dissolved oxygen in UO_2 lattice. The background theory which give the influence of mechanical stress on the chemical diffusion was widely exposed in [9], [11], [12] and [13], and is based on previous works [14]. We recall here the main point used in our calculations. The diffusion coefficient depends on both the mechanical stress and the stress gradient:

$$D = D_0\left[1 - \frac{M_0\eta_{ij}c}{RT}\left(\frac{\sigma_{ij}}{c} + \frac{\partial\sigma_{ij}}{\partial c}\right)\right] \tag{8}$$

where M_0 is the molar mass of the UO_2, η_{ij} is the chemical expansion coefficient, c is the oxygen concentration which is dissolved in UO_2 lattice, σ is the mechanical stress, T is the temperature and R is the universal constant of gases.

We use here a strong coupling between concentration and mechanical stress. The stress locally modifies the diffusion coefficient and the oxygen concentration induces modifications in lattice parameters, which produces additional mechanical stress. Simulations will be made in two steps. The first step is to calculate the stress induced by the connection of U_3O_7 multi-domains layer and UO_2 substrate due to mismatch between their lattices parameters. The second step is to calculate the

diffusion of oxygen in UO_2 in a coupled stress/diffusion model which takes into account the connection mechanical strain.

The model. According to the previous results, we consider a multi-domain of U_3O_7 (composed by a puzzle of simple domains) lying on a UO_2 substrate. The direction (001) in UO_2 is parallel to the direction (010) in U_3O_7, which corresponds to the case a) in Fig. 1. Thus, the $c(U_3O_7)$ direction lies in the plane of the interface. These domains have two different directions for the c-axis. We consider here that the first domain (called "type A") has it's a-axis parallel to the c-axis of the second domain (called "type B"). Fig. 2 shows such a puzzle of multi-domain. Boundaries between these domains are oriented 45° from the principal axes.

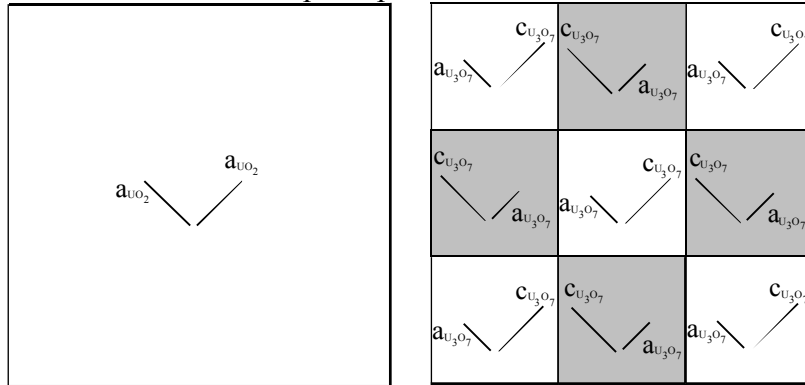Fig. 2. UO_2 and U_3O_7 multi-domain sections: "type A" domains in white and "type B" domains in grey.

In our computations we use FEM code CAST3M. We simulate oxygen diffusion for several thicknesses of U_3O_7 upon infinite UO_2 substrate. *We do not simulate the growth of U_3O_7 layer, but we study influence of a given thickness on diffusion and stresses it induces, both in UO_2 and in U_3O_7 volumes.*

Input parameters. For U_3O_7 material, as it exists mainly in powder form, difficult to characterize, we assumed that the Young modulus and Poisson coefficient are the same as those of UO_2. We consider also that in U_3O_7 the concentration of oxygen is constant and the chemical expansion coefficient can be neglected. The initial conditions are zero oxygen concentration and non-zero mechanical stress (due to the connection between U_3O_7 multi-domain layer and UO_2 substrate). The chemical boundary conditions can be either concentration or flux imposed at the interface U_3O_7/UO_2. The mechanical boundary conditions consist on the elimination of rigid body displacements and on two symmetries to make calculations for only a quarter of the total volume.

Results. An example of connection stress due to the mismatch between lattices parameters of UO_2 and U_3O_7, lying on a section near the frontier U_3O_7/UO_2, is presented in Fig. 3.
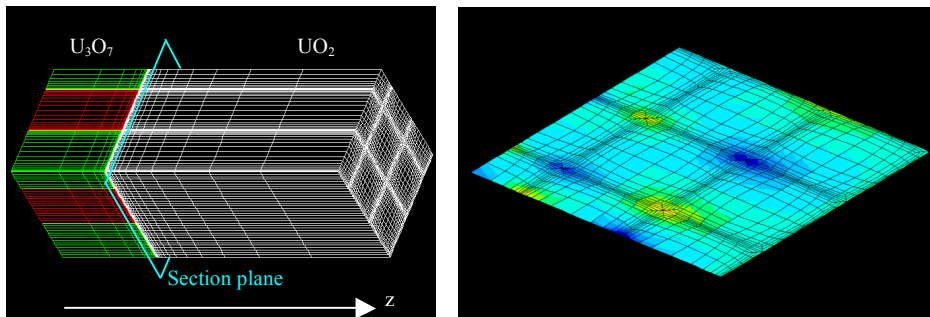

Fig. 3. FEM mesh (left) and σ_{nn} connection stress (right) in a transversal section UO_2 side, at 1 nm from the boundary U_3O_7/UO_2; stress values are from -1 GPa to 1 GPa.

Calculations have been made for several thickness of U_3O_7 layer: the plot of variation of the σ_{xx} stress is shown in Fig. 4. One can see that the maximal value of the stress, U_3O_7 side, is lower for a thickness of 50 nm and 100 nm than for a thickness of 200 nm. It seems to be a confirmation that

stresses in U_3O_7 increase with the thickness of the layer. *We can say that a thick U_3O_7 layer induces maximal traction stress higher than a thin U_3O_7 layer. It can be an explanation of the experimental findings that the U_3O_7 layer cracks when its thickness reaches a critical value.*
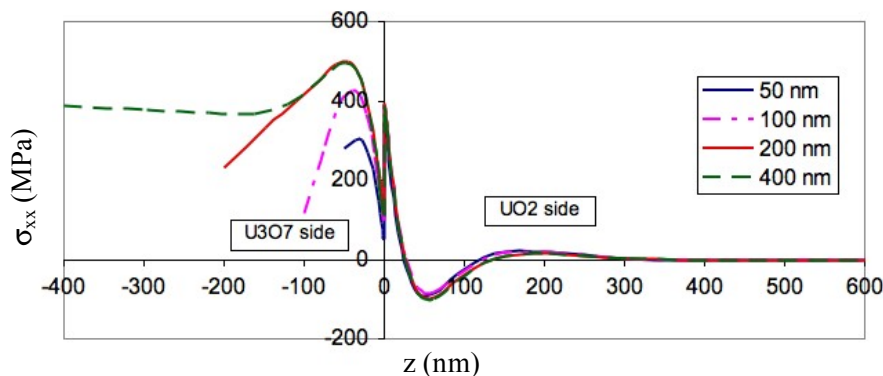

Fig. 4. σ_{xx} stress for several thickness of U_3O_7 layer.

Summary

In this paper, a complete study of the influence of a U_3O_7 domain structure on cracking during the oxidation of UO_2 has been led. The possibility to have a multi-domain structure in the oxide U_3O_7, coexisting with the substrate UO_2, has been shown theoretically thanks to purely geometrical calculations on the crystallographic lattices of the substrate and its oxide (Hadamard relations and Bollmann's method). FEM simulations show, firstly, that the cracking can be due to the multi-domain structure rather than to the sample shape, and secondly, that a critical thickness of the U_3O_7 layer before cracking may exist.

References

[1] K. Bhattacharya, Acta Metall. Mater., Vol. 39 (1991), p. 2431.

[2] L. Hirsinger, N. Creton, C. Lexcellent, J. Phys. IV France, Vol. 115 (2004) pp. 111-120.

[3] W. Breitung, J. Nucl. Mater., Vol. 74 (1978) pp. 10-18.

[4] M. Dodé, B. Touzelin, Revue de Chimie Minérale, Vol. 9 (1972) pp. 139-152.

[5] V. Retel-Guicheret, F. Trivaudey, M.L. Boubakar, Ph. Thevenin, Nucl. Eng. And Design, Vol. 232 (2004) pp. 249-262.

[6] H.R. Hoekstra, A. Santoro, S. Siegel, J. Inorg. Nucl. Chem., Vol. 18 (1961) p. 166.

[7] Y. Saito, Nihon Kinzoku Gakkai-shi. Vol. 39 (1975) p. 760.

[8] W. Bollmann, Springer, Berlin (1970).

[9] I. Salles-Desvignes, T. Montesin, C. Valot, J.Favergeon, G. Bertrand, A. Vadon, Acta Mater., Vol. 38 (2000) pp. 1505-1515.

[10] R. Bonnet, Ph. D. Thesis, Université de Grenoble, France (1974).

[11] J. Favergeon, Ph. D. Thesis, Université de Bourgogne, France (2001).

[12] S. Garruchet, Ph. D. Thesis, Université de Bourgogne, France (2005).

[13] N. Creton, V. Optasanu, T. Montesin, S. Garruchet, L. Desgranges, Defect and Diffusion Forum, Vol. 289-292 (2009) pp. 447-454.

[14] F.C. Larché and J.W. Cahn, Acta Metallurgica, Vol. 30 (1982) pp. 1835-1845.